

p10, the N-terminal domain of p35, protects against CDK5/p25-induced neurotoxicity

Lingyan Zhang^a, Wen Liu^{b,c}, Karen K. Szumlanski^d, and John Lew^{a,1}

^aDepartment of Molecular, Cellular and Developmental Biology and the Neuroscience Research Institute and ^dDepartment of Psychological and Brain Sciences and the Neuroscience Research Institute, University of California, Santa Barbara, CA 93106; and ^bHoward Hughes Medical Institute, and ^cDepartment of Medicine, University of California at San Diego, La Jolla, CA 92093

Edited by John Carbon, University of California, Santa Barbara, CA, and approved October 9, 2012 (received for review August 1, 2012)

Cyclin-dependent kinase 5 (CDK5) in complex with its activator, p35 (protein of 35 kDa), is essential for early neurodevelopment in mammals. However, endogenous cleavage of p35 to p25 is associated with neuron death and neurodegenerative disease. Here we show that a peptide (p10') encoding the N-terminal domain of p35 protects against CDK5/p25-induced toxicity in neurons. p10' also prevented the death of neurons treated with the neurotoxin, 1-methyl-4-phenylpyridinium (MPP⁺), which induces conversion of endogenous p35 to p25, and Parkinson disease (PD)-like symptoms in animals. MPP⁺ induces CDK5/p25-dependent phosphorylation of peroxiredoxin 2 (Prx2), resulting in inhibition of its peroxidoreductase activity and accumulation of reactive oxygen species (ROS). We found that p10' expression inhibited both Prx2 phosphorylation and ROS accumulation in neurons. In addition, p10' inhibited the p25-induced appearance of antigen of the Ki67 antibody (Ki67) and phosphohistone H2AX (γ H2AX), classic markers of cell cycle activity and DNA double-strand breakage, respectively, associated with neuron death. Our results suggest that p10 (protein of 10 kDa) is a unique prosurvival domain in p35, essential for normal CDK5/p35 function in neurons. Loss of the p10 domain results in CDK5/p25 toxicity and neurodegeneration in vivo.

Alzheimer's disease | anti-death

CDK5 (cyclin-dependent kinase 5) kinase activity was originally identified as a tau kinase implicated in Alzheimer's disease (AD) progression (1) and independently as a unique cell cycle kinase homolog exhibiting CDK1-like substrate specificity in brain (2). The active kinase was found to be a heterodimer of CDK5 (3, 4) bound to p25 (5), the latter which was generated from a larger precursor, p35(6–8), by calpain cleavage (9–11). Binding of p35 or p25 (12), or other activators including p39/p29 (13) or cyclin I (14), to CDK5 is essential for protein kinase activity. However, whereas CDK5/p35 is essential for normal embryological development of mammalian brain (15–17), CDK5/p25 induces cell death and is associated with neuropathology (18). Proteolytic conversion of p35 to p25 has been reported to be associated with AD in humans (18, 19) as well as with animal models of Alzheimer's disease (20–22), Parkinson disease (PD) (23, 24), amyotrophic lateral sclerosis (25), and other neurodegenerative disorders.

The relative catalytic activity of CDK5/p35 compared with CDK5/p25 in vivo is not known. In vitro, however, the activities of both enzymes in purified form are equivalent (26). Thus, the simple assumption is that conversion of p35 to p25 does not alter the intrinsic kinase activity of CDK5, and therefore altered kinase activity does not explain the link between p35 cleavage and the toxicity of CDK5/p25. Both enzymes, however, display dramatic differences in subcellular distribution, potentially explaining distinct sets of substrates targeted by either enzyme in vivo (20). For example, CDK5/p35 has reportedly been localized to the cell periphery (18), cytoplasm, and/or nucleus (27, 28) and, in general, targets cytoskeletal, cell adhesion, membrane cycling, axonal transport, synapse, and neuronal migration-related proteins (29). By comparison, CDK5/p25 has been reported to be perinuclear

(18) and nuclear (30) and has been shown to target a number of substrates linked to apoptosis (23, 31–34).

The neurotoxic phenomenon associated with accumulation of p25 has led previous studies to focus exclusively on the mechanism of action of CDK5/p25, whereas the role of the cleaved p35 N-terminal domain (p10) remains unknown. Here we provide evidence that p10 is a unique prosurvival sequence that is essential and alone sufficient to prevent CDK5/p25-induced cell death.

Results

Overexpression of p10' Protects Neurons from Cell Death. Transfection of CDK5/p25 into COS7 (monkey kidney cell line) cells causes chromatin condensation and cell death, in contrast to cells transfected with CDK5/p35 whose nuclei appear normal and healthy (Fig. 1A and ref. 18). Because p25 differs from p35 by only the N-terminal p10 sequence in p35 (6–8), we asked if this sequence when expressed as a separate polypeptide could protect cells from CDK5/p25-induced cell death. We engineered a peptide corresponding to p10 (amino acids 1–98 of p35) fused to the first 40 amino acids of p25 (amino acids 99–138 of p35) so as to accommodate any putative proteins that may potentially require determinants in both p10 and the corresponding region of p25 for binding. The 40-aa segment of p25 does not interact with residues in CDK5 (35) nor does it affect kinase activity (36). The resulting construct, p10' (p35^{1–138}) (Fig. S1), when stably expressed in COS7 cells (Fig. 1A–C) or human SH-SY5Y (human neuroblastoma cell line) neuroblastoma cells (Fig. 1D) completely prevented cellular toxicity induced by CDK5/p25. Transient p10' expression also prevented CDK5/p25-induced cell death in rat primary neurons (Fig. 1E). These experiments reveal a unique function for the p10 domain of p35, which when expressed *in trans* can protect against CDK5/p25-induced cell death in both non-neuronal and neuron-related cell systems.

MPTP is a chemical neurotoxin that induces PD-like symptoms when administered to mammals. The toxicity of 1-methyl-4-phenyl-1,2,3,6-tetrahydropyridine (MPTP) owes to its permeability to the blood–brain barrier followed by its oxidation in glial cells to MPP⁺, the active form of the toxin which targets complex I of the electron transport chain in neurons (37, 38). Electron transport inhibition results in both an energy crisis in the cell and generation of reactive oxygen species (ROS), both of which may contribute to neuron degeneration (39). Interestingly, MPTP causes conversion of endogenous p35 to p25 in neurons of the substantia nigra in mice (31), suggesting that aberrant CDK5/p25 activity may contribute to MPP⁺-induced neurotoxicity.

We found that treatment of neurons with MPP⁺ caused redistribution of anti-p25 staining from being predominantly

Author contributions: L.Z. and J.L. designed research; L.Z. and W.L. performed research; K.K.S. and J.L. contributed new reagents/analytic tools; L.Z. and J.L. analyzed data; and J.L. wrote the paper.

The authors declare no conflict of interest.

This article is a PNAS Direct Submission.

¹To whom correspondence should be addressed. E-mail: lew@lifesci.ucsb.edu.

This article contains supporting information online at www.pnas.org/lookup/suppl/doi:10.1073/pnas.1212914109/-DCSupplemental.

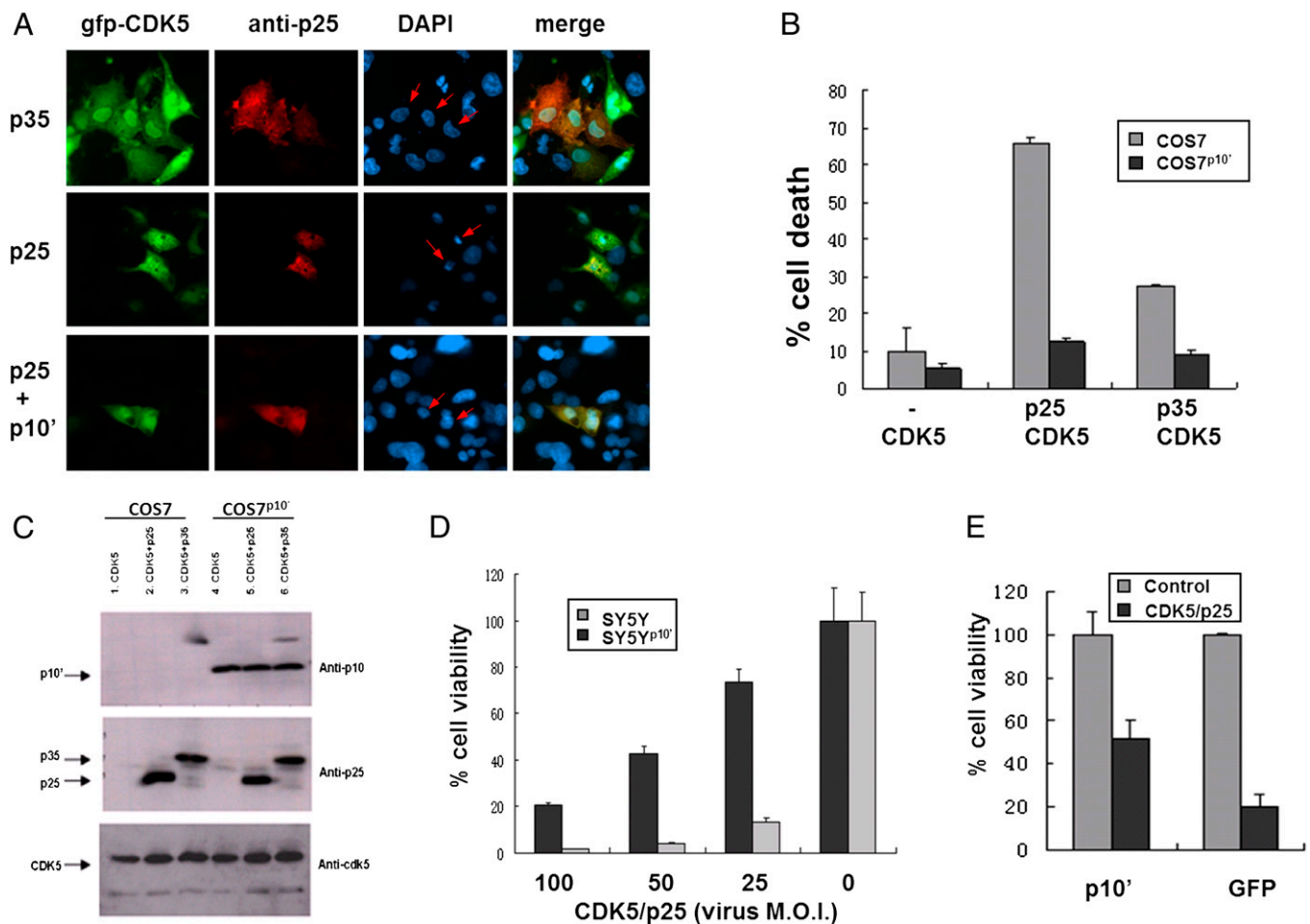


Fig. 1. p10' protects against CDK5/p25 toxicity. (A) COS7 cells were cotransfected with gfp-CDK5 + myc-p35 (Top) or myc-p25 (Middle); COS7 cells stably expressing p10' (COS7^{p10'}) were cotransfected with gfp-CDK5 + myc-p25 (Bottom). Arrows indicate cotransfectants. Mag = 400×. (B) Condensed vs. normal nuclei in A were quantified by counting >300 cells per experimental condition. (C) COS7 or COS7^{p10'} cells were transfected with the indicated genes and Western analysis was conducted on whole cell lysates using the indicated antibodies. (D) SY5Y^{p10'} cells were coinfecting with LV-CDK5 + LV-p25 at decreasing multiplicity of infection (MOI) of both, and cell viability was assessed by using the CellTiter-Glo Assay (Promega) for cellular ATP. (E) Rat primary cortical neurons were infected with LV- p10' or LV-GFP, then subsequently coinfecting with LV-CDK5 + LV-p25. Cell viability was measured 48 h after coinfection by MTT reduction. More than 90% of cells were neurons. All error bars represent SD about the mean from three separate experiments.

membrane-bound to nuclear/perinuclear localization (Fig. S24), followed by cell death. The redistribution is consistent with the normal membrane association of p35 versus the nuclear localization

of p25 when separately overexpressed in COS7 cells (Fig. S2B). Western blot analysis showed that MPP⁺ caused conversion of p35 to p25 within the time frame of subcellular redistribution (Fig. 24).

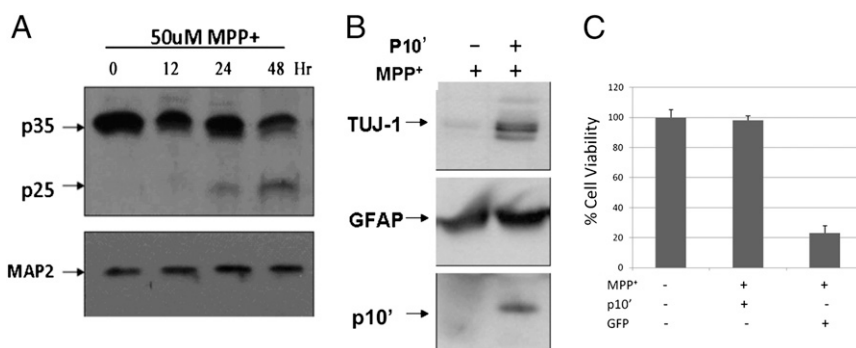


Fig. 2. p10' protects against MPP⁺ toxicity. (A) Rat cortical neurons were treated with 50 μM MPP⁺ for the indicated times, and p25/p35 was visualized by Western blot using anti-p25 (C-19). loading was normalized by anti-MAP2 staining (B) LV-p10' infected or uninfected neurons were treated with MPP⁺ (50 μM), and the presence of live neurons (dead neurons are washed away) was measured after 24 h by neuronal-specific tubulin staining on Western blot using anti-Tuj-1. Anti-GFAP (glial fibrillary acidic protein) shows equal loading (glial cells are not sensitive to MPP⁺); anti-p10 (N-20) shows correlation between cell survival and p10' expression. (C) In the presence of MPP⁺ (50 μM) cell viability was alternatively analyzed by MTT reduction.

Owing to the link between MPP⁺ toxicity and conversion of endogenous p35 to p25, we asked if p10' could protect neurons from MPP⁺ toxicity. MPP⁺ toxicity is classically associated with death of dopaminergic neurons because these neurons specifically concentrate MPP⁺ through the dopamine transporter (40, 41), whereas at higher concentrations, MPP⁺ is also toxic to cortical neurons (23). We found that primary cortical neurons infected with lentivirus (LV)-p10' were significantly protected from MPP⁺ toxicity compared with neurons that were infected with a LV-GFP control protein, measured by the presence of neuronal-specific tubulin (Fig. 2B), which reflects the retention of specifically live neurons in the cell culture well (dead neurons are washed away). Similar results were obtained using a 3-(4,5-dimethylthiazol-2-yl)-2,5-diphenyltetrazolium bromide (MTT) assay, which measures active electron transport (Fig. 2C). The protective action of p10' observed in these experiments is consistent with the possible involvement of CDK5/p25 in MPP⁺ toxicity.

Proteasome Inhibitor MG132 Protects Against Cell Death. Given that p10' can protect against CDK5/p25-induced toxicity, we asked why cleavage of p35 to p25 is associated with neuron death, because p10 is a product of this reaction. We were unable to detect endogenous p10 in neuronal extracts in response to MPP⁺ treatment by Western blot analysis, which led us to hypothesize that p10 may be rapidly degraded. We thus tested if inhibition of the proteasome may promote p10 accumulation. Neurons were treated with the proteasomal inhibitor, MG132. However, under these conditions, endogenous p10 still could not be detected by Western analysis. We thus turned to ask if MG132 may affect the stability of overexpressed p10'. Primary neurons were infected with LV-p10' for 72 h, then treated with MG132 for a further 6 h. During the time of MG132 treatment, p10' was seen to significantly accumulate (Fig. 3A) by Western analysis. This supports but does not prove that endogenous p10 may behave similarly.

To investigate directly the effect of MG132 on endogenous p10, we monitored p10 in neurons by immunocytochemical staining after treatment with MPP⁺ and MG132, either alone or in combination (Fig. 3B). Untreated neurons (control) displayed anti-p10 staining that was localized to the cell periphery and to neuronal processes, consistent with the staining of p35 at the plasma membrane (18). Upon treatment with MPP⁺, anti-p10 staining was effectively abolished, consistent with rapid p10 proteolytic degradation. However, in neurons treated with both MPP⁺ and MG132 together, anti-p10 staining in neuronal processes was preserved, consistent with p35 cleavage and protection of p10 from degradation by MG132. Anti-p25 staining did not track with anti-p10 staining (Fig. 3B, *Insets*), confirming that p35 was cleaved and that the anti-p10 signal was due to p10, not p35. These data suggest that MG132 is not acting via inhibition of p35 cleavage.

Given that MG132 can promote endogenous p10 accumulation in neurons, we tested if MG132 could protect neurons from MPP⁺-induced toxicity. Neurons were observed to undergo significant cell death after 24 h of MPP⁺ treatment. However, when cotreated with both MPP⁺ and MG132, neuron viability was significantly increased (Fig. 3C). These data, in all, strongly suggest that MPP⁺ causes cleavage of CDK5/p35 to generate CDK5/p25 and p10, and in the presence of MG132, p10 accumulates conferring protection of cells from CDK5/p25-associated cell death.

CDK5/p35 and CDK5/p25 display identical kinase activity *in vitro* (26), yet CDK5/p25 is toxic to cells, whereas CDK5/p35 is not. Therefore, it is proposed that p10, which corresponds to the N-terminal domain of p35, intrinsically serves to suppress toxicity in CDK5/p35 in normal neurons. We asked if the neuroprotective activity exhibited by free p10' may be specific to CDK5/p25-associated toxic processes. Staurosporin is toxic to neurons, but its toxicity is not mediated by a CDK5/p25-associated process. When neurons were treated with staurosporin, significant cell death was apparent. However, in contrast to death induced by MPP⁺, p10'

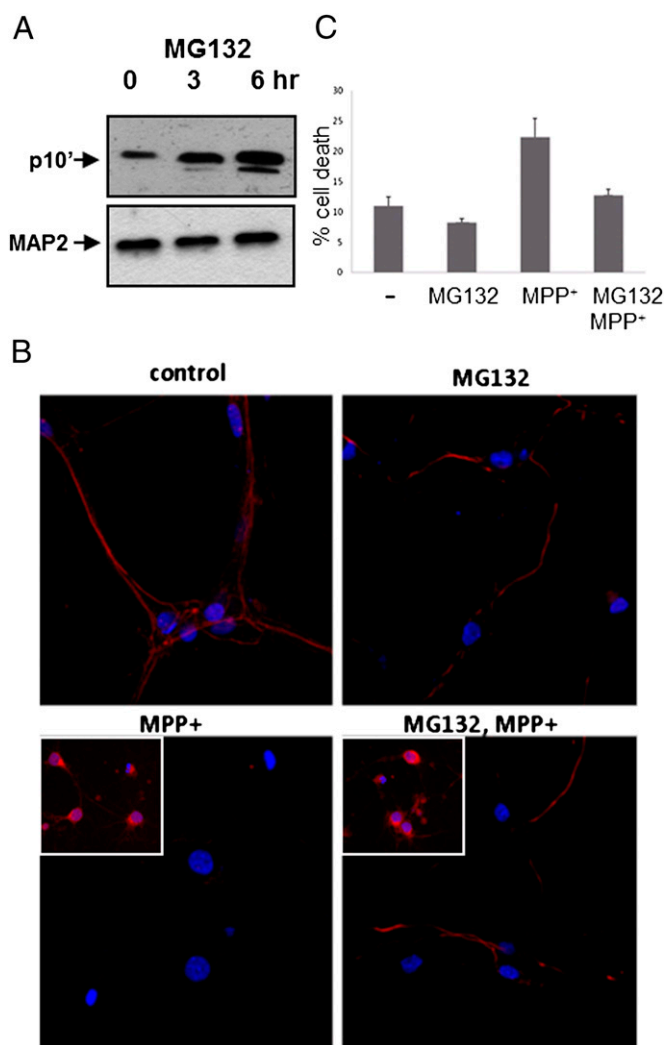


Fig. 3. MG132 protects against MPP⁺ toxicity. (A) Rat cortical neurons were infected for 72 h with LV-p10' at which time p10' expression levels were constant. Neurons were then treated with 10 μ M MG132 for 0, 3, or 6 h. p10' levels were measured by Western blot using anti-p10 (N-20). (B) Uninfected neurons were stained with anti-p10 (N-20) or anti-p25 (C-19) (*Insets*) in the presence of MPP⁺, MG132, or both, and Cy3 (red) second antibody staining was observed by confocal microscopy. Nuclei were stained with DAPI (blue). (C) Neuron death was determined by Guava ViaCount assay for dying cells after a 1-h pretreatment with 10 μ M MG132, followed by a 24-h treatment with 50 μ M MPP⁺.

provided no significant protection to neurons treated with staurosporin (Fig. S3).

Prx2 Phosphorylation and ROS Accumulation Are Attenuated by p10'. ROS have been implicated in neurotoxicity and invoke the need for appropriate scavengers of ROS in neurons for cell survival. Prx2 is a cellular peroxidase that serves as an essential oxygen free-radical scavenger by catalyzing the conversion of H₂O₂ to H₂O (42). Overexpression of Prx2 in neurons protects against MPP⁺ toxicity (23), whereas direct phosphorylation of Prx2 at Threonine 89 (Thr⁸⁹) by CDK5/p25 in response to MPP⁺ treatment inhibits Prx2 activity, contributing to cell death (23). We asked if the protective action of p10' may possibly involve Prx2-dependent ROS scavenging.

We tested the phosphorylation state of Prx2 in neurons using a pThr⁸⁹-specific antibody in response to CDK5/p25 and p10' expression. We found that CDK5/p25 induced the phosphorylation

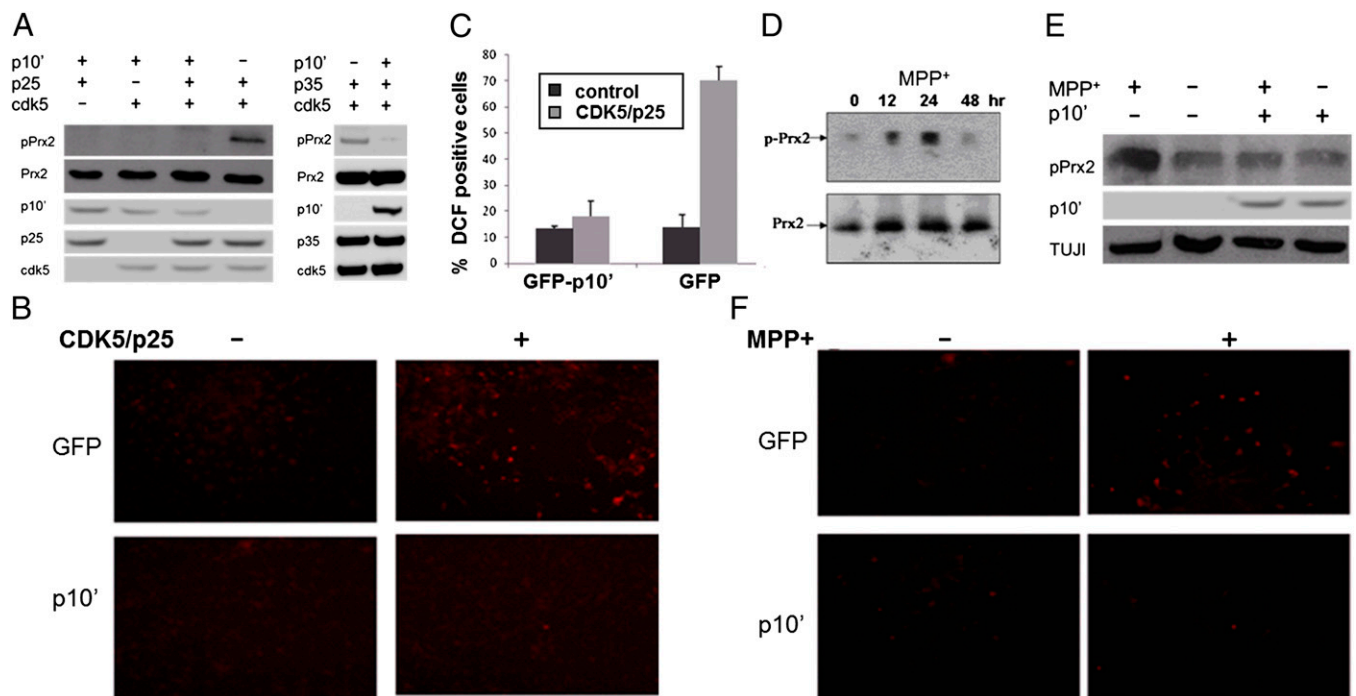


Fig. 4. p10' prevents phosphorylation of Prx2 and generation of reactive oxygen species (ROS) in response to CDK5/p25 or MPP⁺. (A) SH-SY5Y cells were infected with CDK5, p25, or p35 and/or p10' for 48 h. Western analysis was performed on cell lysates using a Prx2-pThr⁸⁹-specific (first row), or Prx2-specific (second row) antibody. (B) ROS production was monitored by DCF staining in cells expressing GFP, p10', CDK5/p25 + GFP, or CDK5/p25 + p10'. (C) DCF fluorescence at 480 nm was quantified by FACS. A total of 5,000 cells per condition were flow sorted using a Guava EasyCyte instrument. (D) Rat cortical neurons were treated with MPP⁺ (50 μ M), and Prx2 phosphorylation at varying times was monitored by Western blot. (E) Neurons were infected with p10' for 48 h, then treated with 50 μ M MPP⁺ for 24 h. Cell lysates were analyzed by Western blot for pPrx2. In the presence of MPP⁺ (lanes 1 and 3), p10' reduced the levels of pPrx2 by 3.2-fold (determined by densitometry). (F) ROS production was monitored by DCF staining, as described in B.

of Prx2 and that this phosphorylation was prevented by expression of p10' (Fig. 4A). In addition, we measured ROS levels by 2',7'-dichlorofluorescein (DCF) fluorescence emission and found that CDK5/p25-dependent Prx2 phosphorylation correlated with increased ROS accumulation. This accumulation of ROS was prevented by p10' (Fig. 4B and C).

We then tested if p10' protected against Prx2 phosphorylation and ROS accumulation when toxicity was induced by MPP⁺. Treatment of control neurons with MPP⁺ resulted in both a time-dependent phosphorylation of Prx2 at Thr⁸⁹ (Fig. 4D) and increased ROS generation (Fig. 4F). In contrast, overexpression of p10' in MPP⁺-treated neurons prevented both Prx2 phosphorylation (Fig. 4E) and ROS accumulation (Fig. 4F). Because a direct correlation between Prx2 activity and neuron survival has previously been demonstrated (23), our finding that p10' can directly modulate the Prx2 pathway points to a possible cellular basis for p10's protective action, although the direct target of p10 remains unknown.

Appearance of Ki67 and γ H2AX Is Prevented by p10'. Neuronal apoptosis has been linked to reactivation of the cell cycle machinery. Accordingly, neurons and postmitotic cells in general actively repress cell cycle control proteins (43), and expression of p25 in mouse forebrain leads to transcriptional alterations in both cell cycle and DNA repair genes (44). We therefore asked if p10' would antagonize the effects of p25 on the appearance of cell cycle and/or DNA repair marker proteins. Rat cortical neurons were infected with p25 or p25 + p10', and the number of neurons expressing the cell cycle marker, Ki67, was counted. In response to p25 expression, Ki67 was significantly up-regulated (Fig. 5A), suggesting that cell cycle activity was induced as expected. In the presence of p10', however, the p25-induced cell cycle activity was suppressed, apparent as a decrease in neuronal Ki67 expression to base-line levels. This suggests that the

ability of p10' to inhibit CDK5/p25-induced cell death may be tightly linked to its ability to inhibit aberrant cell cycle activity.

We found also that p25 induced the phosphorylation of neuronal H2AX, a marker of DNA damage, and that p10' attenuated this phosphorylation (Fig. 5B).

The data, overall, suggests that the known cell death pathways activated by CDK5/p25 can be suppressed by p10', consistent with p10's ability to specifically protect against CDK5/p25-induced neuron death.

Discussion

Cleavage of endogenous p35 to form p25, and demonstration that CDK5/p25 is toxic to neurons, was first described by Patrick et al. (18) followed by others (9–11). Since that time, attention has focused extensively on CDK5/p25, whereas the significance of the N-terminal proteolytic fragment, p10, has not been investigated.

Herein we report that free p10' (Fig. S1) prevents the toxicity induced by CDK5/p25 in neurons, conferring the degree of cell viability normally associated with CDK5/p35. A number of observations suggest that the mechanism of protection by p10' is not a simple reconstitution of p35 function. Principally, Prx2 is phosphorylated by CDK5/p35 in SY5Y cells (Fig. 4A). Further, this phosphorylation is inhibited by p10' (Fig. 4A). Lastly, we have been unable to demonstrate p10' binding to CDK5/p25 despite extensive effort by in vitro pull-down assays. These data suggest that the mechanism of action of p10' may depend upon an intact cellular environment. It is unlikely that the p25 region (p35^{99–138}) of p10' directly disrupts interaction between p25 and CDK5, because these residues in p25 do not interact with CDK5 (35). In addition, the proteasome inhibition experiments suggest that the bona fide 98-aa p10 fragment (p35^{1–98}) itself, when induced to accumulate in cells, is functional (Fig. 3C). The fact that p10' inhibits CDK5/p25 phosphorylation of Prx2 in vivo (Fig. 4A) suggests that the

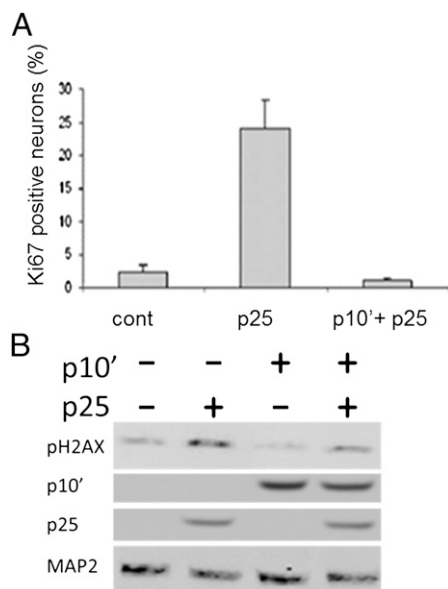


Fig. 5. p10' prevents both Ki67 accumulation and H2AX phosphorylation. (A) Ki67. Neurons were isolated and cultured as described in *Materials and Methods*. Neurons were identified by anti-MAP2 staining. Ki67-expressing cells were identified by anti-Ki67 staining (Fig. S5). Percent of Ki67⁺ neurons in uninfected control, p25, or p10' + p25-infected cells was determined by counting >500 neurons. Values are mean \pm SD, $n = 3$. (B) H2AX. Western blot analysis of whole neurons was performed with the indicated antibodies.

mechanism of action of p10' may depend upon one or more unknown cellular factors. One possibility is the requirement of a cellular factor for formation of an inhibitory complex comprising endogenous p10, p25, CDK5, and possibly Prx2 or another endogenous substrate.

The mechanism by which p10 affects cell viability is not known. Chew et al. reported that p10 is in fact toxic when overexpressed in the neuroblastoma cell line neuro-2A (45). In contrast, we consistently found that p10' had no effect on cell viability when stably expressed in COS7 or SH-SY5Y cells or when transiently expressed in rat cortical neurons. To address this inconsistency directly, we obtained the p10 expression constructs used in the studies of Chew et al. (provided by R. Z. Qi, Hong Kong University of Science and Technology, Hong Kong). Using their constructs, we found that p10 expression was *not toxic* when tested in SH-SY5Y neuronal cells (Fig. S4). In fact, p10 protected against CDK5/p25 toxicity (Fig. S4), consistent with all results that we have observed and which we report herein. The source of the discrepancy between our results and those of Chew et al. (45) remains unknown. Our own data, which show that p10 is a prosurvival sequence, explain how degradation of the N-terminal p10 domain of p35 leads to CDK5/p25 toxicity. On the other hand, if both CDK5/p25 and p10 were intrinsically toxic, as proposed by Chew et al., it is difficult to rationalize how toxicity would be averted in the CDK5/p35 molecule present in normal neurons.

p25 has been implicated in Alzheimer's disease (46, 47), and inhibitors of CDK5/p25 are presently being sought as potential therapeutics of neurodegeneration. Because it is reported that CDK5/p35 may be essential in adult neurons to prevent cell cycle reentry and death (48), it is imperative that an inhibitor molecule effectively discriminates between CDK5 bound to p25 as opposed to p35. However, as with most kinase inhibitors that act competitively with ATP or conceivably the protein substrate, all known conventional inhibitors of CDK5 are expected to target both CDK5/p25 and CDK5/p35, because both enzymes exhibit comparable active site structures based on their similar catalytic efficiencies toward histone or tau protein (26). Our studies herein

suggest that p10 may represent a unique class of CDK5 inhibitor capable of preventing the toxic effects of CDK5/p25 without affecting the normal function of CDK5/p35.

Materials and Methods

Antibodies. C-19 is directed toward the p25 domain of p35 and recognizes p25 or p35. N-20 is directed to the p10 domain of p35 and recognizes p10 or p35. C-19, N-20, C-8 (CDK5), J-3 (CDK5), 9E10 (c-myc) anti-GFAP, anti-MAP2 and anti-GFP are from Santa Cruz. Other antibodies used were: antitubulin (Sigma), anti-Prx2 (monoclonal; Abcam), and Alexa-labeled secondary antibodies (Invitrogen); anti-Ki67 (BD Bioscience); anti- γ H2AX (anti-pH2AX) (Upstate Biotech); Tuj-1 (NeuroMics); anti-IgG (Jackson ImmunoResearch); and anti-TH (Immunostar). Anti-Prx2 (pThr⁸⁹) polyclonal antibody was a gift from David Park, University of Ottawa, Ottawa.

Primary Neuronal Cell Culture. All animal protocols were IACUC approved by the animal resource center at the University of California, Santa Barbara. Whole brains were collected from rat E18 embryos. Forebrains were dissected in medium [1 \times HBSS (Gibco), 10 mL Hepes (pH 7.3), 10 mL 100 \times Pen/Strep (Gibco)], and the meninges and blood vessels were removed. Cortex was then removed from the forebrain and incubated with 25 mg/mL trypsin at 37 $^{\circ}$ C for 10–15 min, then dispersed by repeated aspiration with a Pasteur pipette. After trypsinization, tissue was then homogenized in 10% glial MEM (425 mL MEM; Gibco), 15 mL 20% glucose, 5 mL 100 \times Pen/Strep, and 50 mL horse serum). Cells were counted and plated in 10% glial MEM in Nunc 60-mm dishes (5×10^6 cells per well) for Western blot or on pretreated cover glass (Fisher) ($2\text{--}5 \times 10^5$ cells per well) for immunocytochemistry and survival assay. After neurons were completely seeded, they were maintained in neurobasal media supplemented with B-27 and N2 nutritional supplements, 0.5 mM glutamine, and 0.05 mg/mL pen/strep (all from Invitrogen) for 7–10 d before experimental use. After 3 d in culture, cells were treated with 1 μ M cytosine arabinoside to enrich for neurons by killing proliferative cells.

Forty-eight hours after LV transduction, cultures were subjected to 50 μ M MPP⁺ or DMSO as control. In select experiments, neurons were also pretreated with 10 μ M MG132 (Sigma), the proteasome inhibitor for 1 h, and then cotreated with 20 μ M MPP⁺ or control.

Immunocytochemistry. Cells were transfected with expression vectors, or primary cortical neuronal cells were infected with lentivirus. Efficiency of lentiviral infection was consistently 50–60%. Cells were fixed for 5–15 min with 4% formaldehyde in PBS, then permeabilized for 10 min with 0.1% Triton X-100 in PBS. After three rinses with PBS buffer, blocking solution (5% BSA in PBS, pH 7.4) was applied for 30 min and primary antibodies against p25 (C-19, 1:200; Santa Cruz), p10 (N-20, 1:100; Santa Cruz), c-myc (9E10, 1:500; Santa Cruz), Ki67 (BD Bioscience, 1:200), MAP2 (Santa Cruz, 1:500) were added in blocking buffer for 1 h at room temperature. After 3 \times 5 min washes with PBS, cells were incubated with DAPI and with secondary antibodies conjugated with fluorescent dyes (Invitrogen) for 1 h, washed again with PBS, and mounted in Fluoromount-G (SouthernBiotech). Images were recorded on a high-resolution fluorescence microscope (Olympus BX 51) equipped with MicroFire camera. Confocal imaging was performed on an Olympus Fluoview FV500 microscope using an Olympus UPLFLN 40 \times NA = 1.3 oil-immersion objective. Z stacks (0.2- μ m sections) were deconvoluted using softWoRx (Applied Precision), projected for maximum intensity and imported into Adobe Photoshop CS4 for further processing. Image intensities for each antibody were scaled identically.

Cell Viability Assay. After immunostaining, COS7 cells were labeled with the DNA dye DAPI (Invitrogen), and double-transfected COS7 cells were scored for healthy or apoptotic nuclear morphology. Cells were scored positive if they had a pyknotic and/or fragmented nucleus. Representative graphs are shown for experiments where 150 or 300 cells were scored. All experiments were done at least three times.

Neuronal cell viability was measured by reduction of MTT or by Guava ViaCount viability assay. The MTT assay was performed by adding MTT (0.5 mg/100 μ L per well) to each well, followed by incubation for 10 min at 37 $^{\circ}$ C under 5% CO₂. At the end of the assay, 1 mL of DMSO was added to each well to extract the formazan produced. Formazan was measured by absorbance at 540 nm.

For Guava ViaCount viability assay, 225 μ L of ViaCount reagent was added to 25 μ L of cell suspension (1×10^5 cells/mL). The cells were stained for at least 5 min and the viability measured by Guava EasyCyte Flow Cytometry (Millipore).

Cell viability of SH-SY5Y cells was measured by using CellTiter-glo Luminescent Cell Viability Assay kit (Promega) following manufacturer protocol. Briefly, cells were plated in 96-well plates at a density of 1×10^3 per well. A

total of 50 μ L of reagent was added into per 50 μ L of culture medium with cells. The culture plates were incubated at room temperature for 10 min. The luminescent signal was measured with a microplate reader.

Reactive Oxygen Species Imaging. Cortical neurons were incubated with 10 mM H₂DCFDA-AM for 20 min at 37 °C and washed three times with neurobasal (NB) medium. The fluorescence signal of the oxidized product

DCF (2',7'-dichlorodihydrofluorescein) was observed by an inverted fluorescent microscope equipped with a 100 W xenon lamp and filter (for oxidized DCF, excitation = 488 nm and emission = 510 nm). DCF⁺ cells were quantified by Guava EasyCyte Flow Cytometry (Millipore).

ACKNOWLEDGMENTS. This work was supported by National Institutes of Health Grant GM058445.

1. Ishiguro K, et al. (1992) Tau protein kinase I converts normal tau protein into A68-like component of paired helical filaments. *J Biol Chem* 267(15):10897–10901.
2. Lew J, Beaudette K, Litwin CM, Wang JH (1992) Purification and characterization of a novel proline-directed protein kinase from bovine brain. *J Biol Chem* 267(19):13383–13390.
3. Kobayashi S, et al. (1993) A cdc2-related kinase PSSALRE/cdk5 is homologous with the 30 kDa subunit of tau protein kinase II, a proline-directed protein kinase associated with microtubule. *FEBS Lett* 335(2):171–175.
4. Lew J, Winkfein RJ, Paudel HK, Wang JH (1992) Brain proline-directed protein kinase is a neurofilament kinase which displays high sequence homology to p34cdc2. *J Biol Chem* 267(36):25922–25926.
5. Ishiguro K, et al. (1994) Identification of the 23 kDa subunit of tau protein kinase II as a putative activator of cdk5 in bovine brain. *FEBS Lett* 342(2):203–208.
6. Lew J, et al. (1994) A brain-specific activator of cyclin-dependent kinase 5. *Nature* 371(6496):423–426.
7. Tsai LH, Delalle I, Caviness VS, Jr., Chae T, Harlow E (1994) p35 is a neural-specific regulatory subunit of cyclin-dependent kinase 5. *Nature* 371(6496):419–423.
8. Uchida T, et al. (1994) Precursor of cdk5 activator, the 23 kDa subunit of tau protein kinase II: Its sequence and developmental change in brain. *FEBS Lett* 355(1):35–40.
9. Kusakawa G, et al. (2000) Calpain-dependent proteolytic cleavage of the p35 cyclin-dependent kinase 5 activator to p25. *J Biol Chem* 275(22):17166–17172.
10. Lee MS, et al. (2000) Neurotoxicity induces cleavage of p35 to p25 by calpain. *Nature* 405(6784):360–364.
11. Nath R, et al. (2000) Processing of cdk5 activator p35 to its truncated form (p25) by calpain in acutely injured neuronal cells. *Biochem Biophys Res Commun* 274(1):16–21.
12. Qi Z, Huang QQ, Lee KY, Lew J, Wang JH (1995) Reconstitution of neuronal Cdc2-like kinase from bacteria-expressed Cdk5 and an active fragment of the brain-specific activator. Kinase activation in the absence of Cdk5 phosphorylation. *J Biol Chem* 270(18):10847–10854.
13. Hisanaga S, Saito T (2003) The regulation of cyclin-dependent kinase 5 activity through the metabolism of p35 or p39 Cdk5 activator. *Neurosignals* 12(4-5):221–229.
14. Brinkkoetter PT, Pippin JW, Shankland SJ (2010) Cyclin I-Cdk5 governs survival in post-mitotic cells. *Cell Cycle* 9(9):1729–1731.
15. Cruz JC, Tsai LH (2004) A Jekyll and Hyde kinase: Roles for Cdk5 in brain development and disease. *Curr Opin Neurobiol* 14(3):390–394.
16. Gupta A, Tsai LH (2003) Cyclin-dependent kinase 5 and neuronal migration in the neocortex. *Neurosignals* 12(4-5):173–179.
17. Dhavan R, Tsai LH (2001) A decade of CDK5. *Nat Rev Mol Cell Biol* 2(10):749–759.
18. Patrick GN, et al. (1999) Conversion of p35 to p25 deregulates Cdk5 activity and promotes neurodegeneration. *Nature* 402(6762):615–622.
19. Nguyen KC, Rosales JL, Barboza M, Lee KY (2002) Controversies over p25 in Alzheimer's disease. *J Alzheimers Dis* 4(2):123–126.
20. Cruz JC, Tsai LH (2004) Cdk5 deregulation in the pathogenesis of Alzheimer's disease. *Trends Mol Med* 10(9):452–458.
21. Oth T, et al. (2002) AbetaPP induces cdk5-dependent tau hyperphosphorylation in transgenic mice Tg2576. *J Alzheimers Dis* 4(5):417–430.
22. Lau LF, Ahljianian MK (2003) Role of cdk5 in the pathogenesis of Alzheimer's disease. *Neurosignals* 12(4-5):209–214.
23. Qu D, et al. (2007) Role of Cdk5-mediated phosphorylation of Prx2 in MPTP toxicity and Parkinson's disease. *Neuron* 55(1):37–52.
24. Smith PD, et al. (2003) Cyclin-dependent kinase 5 is a mediator of dopaminergic neuron loss in a mouse model of Parkinson's disease. *Proc Natl Acad Sci USA* 100(23):13650–13655.
25. Nguyen MD, Larivière RC, Julien JP (2001) Deregulation of Cdk5 in a mouse model of ALS: Toxicity alleviated by perikaryal neurofilament inclusions. *Neuron* 30(1):135–147.
26. Peterson DW, et al. (2010) No difference in kinetics of tau or histone phosphorylation by CDK5/p25 versus CDK5/p35 in vitro. *Proc Natl Acad Sci USA* 107(7):2884–2889.
27. Fu X, et al. (2006) Identification of nuclear import mechanisms for the neuronal Cdk5 activator. *J Biol Chem* 281(51):39014–39021.
28. Asada A, et al. (2008) Myristoylation of p39 and p35 is a determinant of cytoplasmic or nuclear localization of active cyclin-dependent kinase 5 complexes. *J Neurochem* 106(3):1325–1336.
29. Guo Q (2006) When good Cdk5 turns bad. *Sci SAGE KE* 2006(5):pe5.
30. O'Hare MJ, et al. (2005) Differential roles of nuclear and cytoplasmic cyclin-dependent kinase 5 in apoptotic and excitotoxic neuronal death. *J Neurosci* 25(39):8954–8966.
31. Smith PD, et al. (2006) Calpain-regulated p35/cdk5 plays a central role in dopaminergic neuron death through modulation of the transcription factor myocyte enhancer factor 2. *J Neurosci* 26(2):440–447.
32. Tian B, Yang Q, Mao Z (2009) Phosphorylation of ATM by Cdk5 mediates DNA damage signalling and regulates neuronal death. *Nat Cell Biol* 11(2):211–218.
33. Maestre C, Delgado-Esteban M, Gomez-Sanchez JC, Bolaños JP, Almeida A (2008) Cdk5 phosphorylates Cdh1 and modulates cyclin B1 stability in excitotoxicity. *EMBO J* 27(20):2736–2745.
34. Lee JH, Kim HS, Lee SJ, Kim KT (2007) Stabilization and activation of p53 induced by Cdk5 contributes to neuronal cell death. *J Cell Sci* 120(Pt 13):2259–2271.
35. Tarricone C, et al. (2001) Structure and regulation of the CDK5-p25(nck5a) complex. *Mol Cell* 8(3):657–669.
36. Amin ND, Albers W, Pant HC (2002) Cyclin-dependent kinase 5 (cdk5) activation requires interaction with three domains of p35. *J Neurosci Res* 67(3):354–362.
37. Tipton KF, Singer TP (1993) Advances in our understanding of the mechanisms of the neurotoxicity of MPTP and related compounds. *J Neurochem* 61(4):1191–1206.
38. Przedborski S, Jackson-Lewis V (1998) Mechanisms of MPTP toxicity. *Mov Disord* 13(Suppl 1):35–38.
39. Hirsch EC (1999) Mechanism and consequences of nerve cell death in Parkinson's disease. *J Neural Transm Suppl* 56:127–137.
40. Javitch JA, Snyder SH (1984) Uptake of MPP(+) by dopamine neurons explains selectivity of parkinsonism-inducing neurotoxin, MPTP. *Eur J Pharmacol* 106(2):455–456.
41. Javitch JA, Uhl GR, Snyder SH (1984) Parkinsonism-inducing neurotoxin, N-methyl-4-phenyl-1,2,3,6-tetrahydropyridine: Characterization and localization of receptor binding sites in rat and human brain. *Proc Natl Acad Sci USA* 81(14):4591–4595.
42. Rhee SG, Yang KS, Kang SW, Woo HA, Chang TS (2005) Controlled elimination of intracellular H₂O₂: Regulation of peroxiredoxin, catalase, and glutathione peroxidase via post-translational modification. *Antioxid Redox Signal* 7(5-6):619–626.
43. Becker EB, Bonni A (2004) Cell cycle regulation of neuronal apoptosis in development and disease. *Prog Neurobiol* 72(1):1–25.
44. Kim D, et al. (2008) Deregulation of HDAC1 by p25/Cdk5 in neurotoxicity. *Neuron* 60(5):803–817.
45. Chew J, et al. (2010) Identification of p10 as a neurotoxic product generated from the proteolytic cleavage of the neuronal Cdk5 activator. *J Cell Biochem* 111(5):1359–1366.
46. Cruz JC, Tseng HC, Goldman JA, Shih H, Tsai LH (2003) Aberrant Cdk5 activation by p25 triggers pathological events leading to neurodegeneration and neurofibrillary tangles. *Neuron* 40(3):471–483.
47. Noble W, et al. (2003) Cdk5 is a key factor in tau aggregation and tangle formation in vivo. *Neuron* 38(4):555–565.
48. Zhang J, et al. (2010) Cdk5 suppresses the neuronal cell cycle by disrupting the E2F1-DP1 complex. *J Neurosci* 30(15):5219–5228.